A patchy horizontal organization of the somatosensory activation of the rat cerebellum demonstrated by functional MRI

R. R. Peeters, M. Verhoye, B. P. Vos,[2] D. Van Dyck,[1] A. Van Der Linden and E. De Schutter[2]

Bio Imaging Lab, University of Antwerp, RUCA, Belgium, [1]Vision Lab, University of Antwerp, RUCA, Belgium, [2]Laboratory for Theoretical Neurobiology, Born-Bunge Foundation, University of Antwerp-UIA, Universiteitsplein 1, B2610 Antwerp, Belgium

Abstract

Blood oxygenation level dependent contrast (BOLD) functional MRI (fMRI) responses, in a 7-T magnet, were observed in the cerebellum of alpha-chloralose anaesthetized rats in response to innocuous electrical stimulation of a forepaw or hindpaw. The responses were imaged in both coronal and sagittal slices which allowed for a clear delineation and localization of the observed activations. We demonstrate the validity of our fMRI protocol by imaging the responses in somatosensory cortex to the same stimuli and by showing reproducibility of the cerebellar responses. Widespread bilateral activations were found with mainly a patchy and mediolateral band organization, more pronounced ipsilaterally. Possible parasagittal bands were observed only in contralateral lobule VI. There was no overlap between the cerebellar activations caused by forepaw and hindpaw stimuli. The overall horizontal organization of these responses was quite remarkable. For both stimulation paradigms most of the activation patches were positioned in either a rostral or caudal broad plane running anteroposteriorly through both anterior and posterior cerebellum. The rostral planes were completely separated, with the forepaw activation closer to the surface, while the caudal plane was common to both stimulation protocols. We relate our findings to the known projection patterns of spinocerebellar and cuneocerebellar mossy fibres, and to human fMRI studies.

Introduction

The cerebellum receives afferent input from both mossy fibres and climbing fibres, but these two major types of input are organized quite differently (Hawkes, 1997). The climbing fibre projection from the inferior olivary nucleus has a well-defined parasagittal organization (Sasaki *et al.*, 1989; Voogd, 1995; De Zeeuw *et al.*, 1996), while the mossy fibre system, which arises from many sources including spinal cord and corticopontine projections, has a patchy, fractured somatotopy in the cerebellar hemispheres (Shambes *et al.*, 1978; Bower *et al.*, 1981; Welker, 1987). The anatomical topography of the spinal cord mossy fibre projections to the rat cerebellum is well known (Tolbert *et al.*, 1993; Voogd, 1995; Tolbert & Gutting, 1997), but that of the corticopontine projection is not, despite the fact that it is among the largest projection systems in the brain (Brodal & Bjaalie, 1997).

Functional brain mapping methods (Ogawa *et al.*, 1990a,b) allow one to study the activation of specific projections to the entire brain at once. The most commonly used functional MRI (fMRI) technique is blood oxygenation-level-dependent contrast (BOLD), where a change in concentration of the blood's own deoxyhemoglobin manifests itself in a small change in signal intensity in T_2^*-weighted images (Ogawa *et al.*, 1990a; Turner *et al.*, 1991). Due to its noninvasiveness, the BOLD-fMRI technique has become very popular in studies of the human brain. These include both high-resolution imaging of the

functional topography of visual (Tootell *et al.*, 1996) and somatosensory cortex (Sakai *et al.*, 1995) and the determination of brain areas involved in specific cognitive tasks, like learning of motor control (Karni *et al.*, 1995) or speech production (Binder, 1997).

Reports on animal fMRI studies on the other hand are sparse and have mostly used simple stimulation protocols, measuring well-defined input projections to the cortex in the rat (Hyder *et al.*, 1994; Gyngell *et al.*, 1996; Kerskens *et al.*, 1996; Yang *et al.*, 1996, 1997), the mouse (Huang *et al.*, 1996) or the cat (Jezzard *et al.*, 1997). While the cerebellum is receiving particular attention in fMRI studies of the human brain (Ellerman *et al.*, 1994; Gao *et al.*, 1996; Allen *et al.*, 1997; Desmond & Fiez, 1998), imaging studies in animals have been limited to the optical recordings of voltage changes at the surface of the cerebellum only (Ebner & Chen, 1995; Chen *et al.*, 1996; Cohen & Yarom, 1998). Nevertheless, as the function of the cerebellum is at present quite controversial (De Schutter & Maex, 1996; Raymond *et al.*, 1996; Bower, 1997; Schmahmann, 1997), it is important to image the functional activation of the cerebellum in animals, where the results can be compared with the extensive anatomy and electrophysiology available.

Because of the limited sampling typical of anatomical or electrophysiological techniques, projections to only a few parts of the rat cerebellum have been mapped in detail (Welker, 1987; Voogd, 1995). FMR imaging could be an efficient method to map the functional projections everywhere in the cerebellum at once, provided it can achieve the necessary resolution to image patches which often have a diameter of only a few 100 µm. In this study we demonstrate the possibility of mapping functional activation in the rat cerebellum

using fMRI in a 7-T magnet, which allows for a resolution of $\approx 200\,\mu m$ (Hyder *et al.*, 1994). We demonstrate that the observed patchy activation patterns have an overall horizontal organization.

Our results have been reported previously in abstract form (Peeters *et al.*, 1998).

Materials and methods

Animal preparation

Nine adult female wistar rats (200–300 g) were initially sedated with a subcutaneous injection containing a mixture of ketamine (35 mg/kg, Ketalar, Parke-Davis, Belgium) and xylazine (5 mg/kg, Rompun, Bayer, Germany). After 10 min, alpha-chloralose (40 mg/kg, Acros Organics, Belgium) was administrated i.p. and a supplemental dose (30 mg/kg i.p.) was given 2 h later. Anaesthesia waned after 3 h, often leading to movement artifacts. The animal was fixed in a plexiglass stereotactic head holder, consisting of an incisor bar and blunt earplugs, to enable accurate positioning within the magnet and immobilization of the animal. During the experiment, the respiration rate of the animal was monitored and the body temperature was maintained using a warm water blanket ($37 \pm 1\,°C$). The experimental procedures were approved by the Ethical Committee of the University of Antwerp, in accordance with Federal laws.

A copper wire, which was covered with a conductive electrode paste (GRASS, Astro-Med, West Warwick, USA), was wrapped with a single turn around the left forepaw and a second wire was attached similarly to the left hindpaw. Square electrical pulses (WPI stimulator, Sarasota, FL, USA) were delivered with a frequency of 2.5 Hz and a duration of 0.5 ms, resulting in a duty cycle of 0.125%. The current amplitude was 200 μA, which is considered to be innocuous (Handwerker & Kobal, 1993).

MRI methods

MRI was performed at 300 MHz on a SMIS MR microscope (SMIS, Guilford, UK) with a horizontal 7-T magnet and 8-cm-aperture self-shielded gradient coils with a gradient strength of 0.1 T/m (Oxford Instruments, UK). A circular RF surface coil of 16 mm diameter was placed on top of the skull and was used for both transmitting and receiving the MR signal.

To image the cerebral cortex, the surface coil was positioned with its centre ≈ 1 mm posterior to the bregma, and 12 coronal images with a slice thickness of 1 mm were taken from 4 mm anterior to 7 mm posterior to the bregma. To image the cerebellum, the surface coil was placed over the cerebellum with the centre of the coil ≈ 3 mm posterior to the interaural line. Twelve coronal or sagittal slices of 1 mm were imaged, covering the complete cerebellum.

All images were acquired with a multislice gradient echo (GE) sequence. After tuning and shimming (^{1}H linewidth of ≈ 40 Hz), high-resolution sagittal and coronal images were taken, with a field of view (FOV) of 20 mm, a gradient echo time (TE) of 8 ms, a repetition time (TR) of 500 ms and an acquisition matrix of 256×128. Two averages were taken and all images were reconstructed after zero-filling the acquisition matrix to 256×256 data points.

Coronal and sagittal multislice fMRI was performed at the same position of the six inner slices of the high-resolution coronal images or the eight inner slices of the high-resolution sagittal ones. The GE-sequence was T_2^*-weighted (TE = 16 ms, slice thickness = 1 mm, FOV = 20 mm, image matrix = 128×128) with a TR of 150 ms for the coronal and 200 ms for the sagittal images. The total acquisition time per image set was 19.2 s for

the coronal and 25.6 s for the sagittal images. The spatial resolution of the functional images was $160 \times 160\,\mu m$.

Stimulation protocol

The stimulation protocol for all the animals consisted of three cycles of six images without and six images with stimulation of one of the paws, resulting in 36 functional image sets. Figure 1 shows the protocol and the resulting signal intensity changes in different areas. This protocol was used for both forepaw and hindpaw stimulation. In most rats two consecutive protocols were executed: either one orientation of slicing for both paws or both orientations for one paw. In a few rats all four stimulation protocols were executed, but movement artifacts in the last parts of the experiment corrupted the last set of images in all except one (rat 5).

Data analysis

The fMRI data were analysed off-line using both routines in MEDx (Version 3.0, Sensor Systems, Sterling, USA) and custom developed routines and procedures in IDL (Interactive Data Language, RSI, Boulder, CO, USA). The following steps were taken to obtain the activation maps. (i) A motion-detection algorithm, detecting motion of the centre of intensity in three directions was used to assess for major motion artefacts. The motion occurring in the time series was generally found to be at subpixel level, so that no motion correction was necessary. If the motion was higher, some images were discarded from the dataset (only in Fig. 4A, below). (ii) A 3×3 pixel Gaussian convolution filter was applied which resulted in noise reduction of the images. (iii) The activated regions were defined by using a paired *t*-test comparison of the 'stimulation' and 'nonstimulation' images. This resulted in statistical maps giving the *t*-values of each voxel. (iv) This statistical map was interpolated to a 256×256 matrix. (v) The activated regions sustained when thresholding the *t*-values maps at a level of $t(34) = 2$ ($P = 0.05$, giving a confidence level of 95%) were overlaid on the corresponding high-resolution images, resulting in high-resolution images showing in colour the regions with a significant difference between the images acquired with and without stimulation (e.g. Fig 2). (vi) Activation sites were
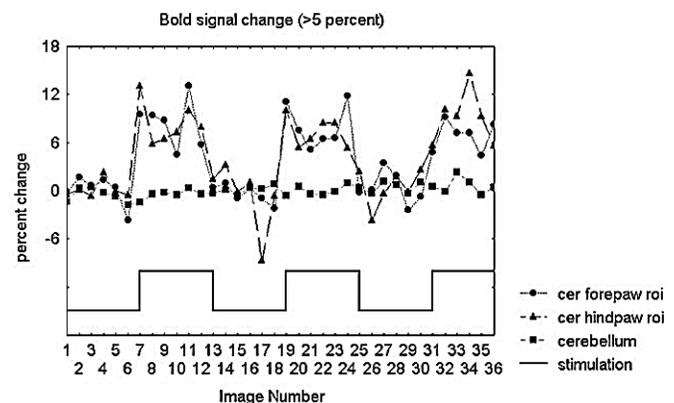

FIG. 1. Time course of the signal change in different regions of interest (roi), during the fMRI experiments with stimulation of the rat's forepaw or hindpaw. The square wave shows the stimulation time course, with the stimulus switching on/off after every six images. The three traces are of from different regions of interest following different stimuli. During hindpaw (▲) and forepaw (●) stimulation, we observed a 6–9% signal change in each corresponding region of interest in the cerebellum. The time course of the signal in the whole cerebellum (■) during stimulation of the hindpaw, produced no significant signal drift.
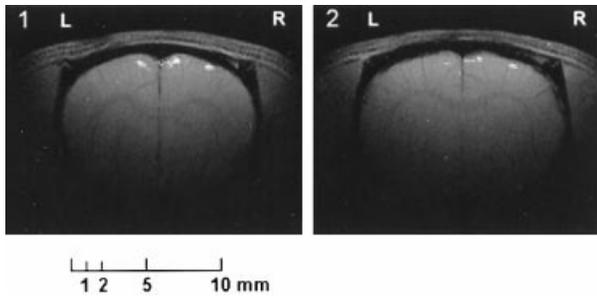
FIG. 2. Cerebral activation maps of two consecutive coronal slices resulting from electrical stimulation of the left forepaw. Activation is shown as brighter spots superposed on the underlying anatomical images. The activations seen near the midline between the two hemispheres are due to a large venous blood vessel; the sagittal sinus and, in the first image, a large contributing vein on the left side. This was confirmed independently by MRI angiography.

identified according to the stereotaxic atlas of the rat brain of Paxinos & Watson (1986).

Results

First, we demonstrate the validity of our fMRI protocol by reproducing imaging results obtained by others in the cerebral cortex (Hyder *et al.*, 1994; Gyngell *et al.*, 1996), then we describe the cerebellar activations.

Activations in somatosensory cortex

Figure 2 shows an example of the activity recorded in two consecutive slices during left forepaw stimulation. Two activation zones were observed: several patches in the midline region between the two hemispheres and one in the right parietal cortex. The midline activations close to the cortical surfaces were due to the presence of the sagittal sinus. It is known that large venous blood vessels are a cause of artefactual signal changes in BOLD imaging (Ogawa *et al.*, 1990a,b; Segebarth *et al.*, 1994). The activation site in the right parietal cortex was in agreement with other studies (Hyder *et al.*, 1994; Gyngell *et al.*, 1996) and with the known location of the forelimb cortex in rat (Chapin & Lin, 1990).

Similarly, during stimulation of the left hindpaw, activation was observed in an area corresponding to the hindpaw area in the right parietal cortex, as expected (Chapin & Lin, 1990) more medial and posterior than the forepaw activation (not shown). These activation patterns were observed in all animals, with small variations probably due to differences in the positioning of the slices between animals.

Activations in the cerebellar cortex

The cerebellar activation patterns caused by stimulation of the hindpaw or forepaw were quite complex; they consisted of many isolated patches, generally organized in a mediolateral fashion. Before describing the activations in detail, we will first consider the validity of our fMRI protocol. The observed activations had *t*-values in the range 2–4.5, indicating high significance levels. Moreover, almost all of the activation spots consisted of several pixels and most of them could be found in both the coronal and sagittal slices.

Figure 3 shows a composite of all the cerebellar activations observed during either left forepaw or left hindpaw activation in a total of nine different rats. This figure demonstrates two important points. First, the pattern of activations we observed was quite reproducible from animal to animal, but individual patches often had slightly different localizations. Secondly, the activations caused by

either front or hindpaw stimulation were almost completely nonoverlapping, both in the coronal and sagittal slices. It is thus unlikely that these cerebellar activations were caused by large venous blood vessels (with an exception possibly in Fig. 5D, see below), like those we found in the cortical images (Fig. 2). The reproducibility and stimulus-dependency of the activations both argue for the validity of our results.

Finally, the original data (Figs 4 and 5) show that the cerebellar activation could not be imaged completely with the surface coil we used. In effect, the area which could be observed reliably was limited to a distance of ≈ 6 mm deep in the coronal slices and 3 mm lateral of the midline in the sagittal slices. Beyond these distances some activations could still be recorded in a reproducible way, but they could not be resolved accurately (e.g. Fig. 5A and C).

While almost no overlapping activations were found for the hind- and forepaw stimuli, they did show many common features. In each case the activations were bilateral, showed a predominantly mediolateral organization and were confined to similar horizontal levels in the anterior and posterior cerebellum. We will next describe the patchy structure in greater detail, based on the original data sets of three rats (Figs 4 and 5). Additional original data can be viewed at http://www.cerebellum.org/fmri.

Cerebellar activation caused by left hindpaw stimulation

As this is the simpler of the two response patterns, we will first consider the response to hindpaw activation in two rats in detail (Fig. 4). In every animal, we observed bilateral signal changes in all the coronal slices through the cerebellum during electrical stimulation. These were situated in a broad horizontal rostral band between 1.5 and 3 mm below the upper surface of the cerebellum (top of VIa), with a few additional activations very deep (≈ 7 mm down).

One of these deep activations was in the anterior cerebellum, where a bilateral activation is observed in lobule I in the sagittal images of most animals (B2–4 and D2–4). It is not observed in the coronal slices, probably because of the large distance from the surface coil. At a similar depth, but more laterally, a large contralateral activation is seen in one animal (B1). In the coronal slices several corresponding activations are situated in the anterior interpositus and lateral nuclei (A2 and C2).

A second series of anterior cerebellum activations is situated around the preculminate fissure. The most anterior one consists, in rat 5, of a number of ipsilateral (three spots in A1 and one in each of B4 and B5) and one contralateral activation in lobule III (A1 and B3). In rat 4, similar activations could be found in the coronal slice C1, but in the sagittal slices only a contralateral activation is visible in D1 and D2. At the other side of the preculminate fissure a series of bilateral activations is observed deep in lobule IV. In rat 5 these are discrete spots just behind and at about the same height as the activations in lobule III (B2–6, but mostly contralateral in A2). In rat 4 the corresponding activations are much more extensive and seem to consist of several confluent patches in the sagittal images (D1–6) and in the coronal image (C2), with a medial extension into lobule V, which is only visible in the sagittal slices (D3 and 4).

Several more lateral spots of activation seen in the coronal slices were outside the field of view for the sagittal slices, so they could not be located accurately. They were probably located in the lobulus simplex or crus I (ipsilateral in C1 and bilateral in A2 and C2, also ipsilateral in B6 and D5) or the top of crus II (bilateral A3 and C3), though a location in the lateral nuclei cannot be excluded. The most noticeable aspect of these activations, combined with the ones described before in lobules III and IV, was their mediolateral organization along a single band (Fig. 3A).
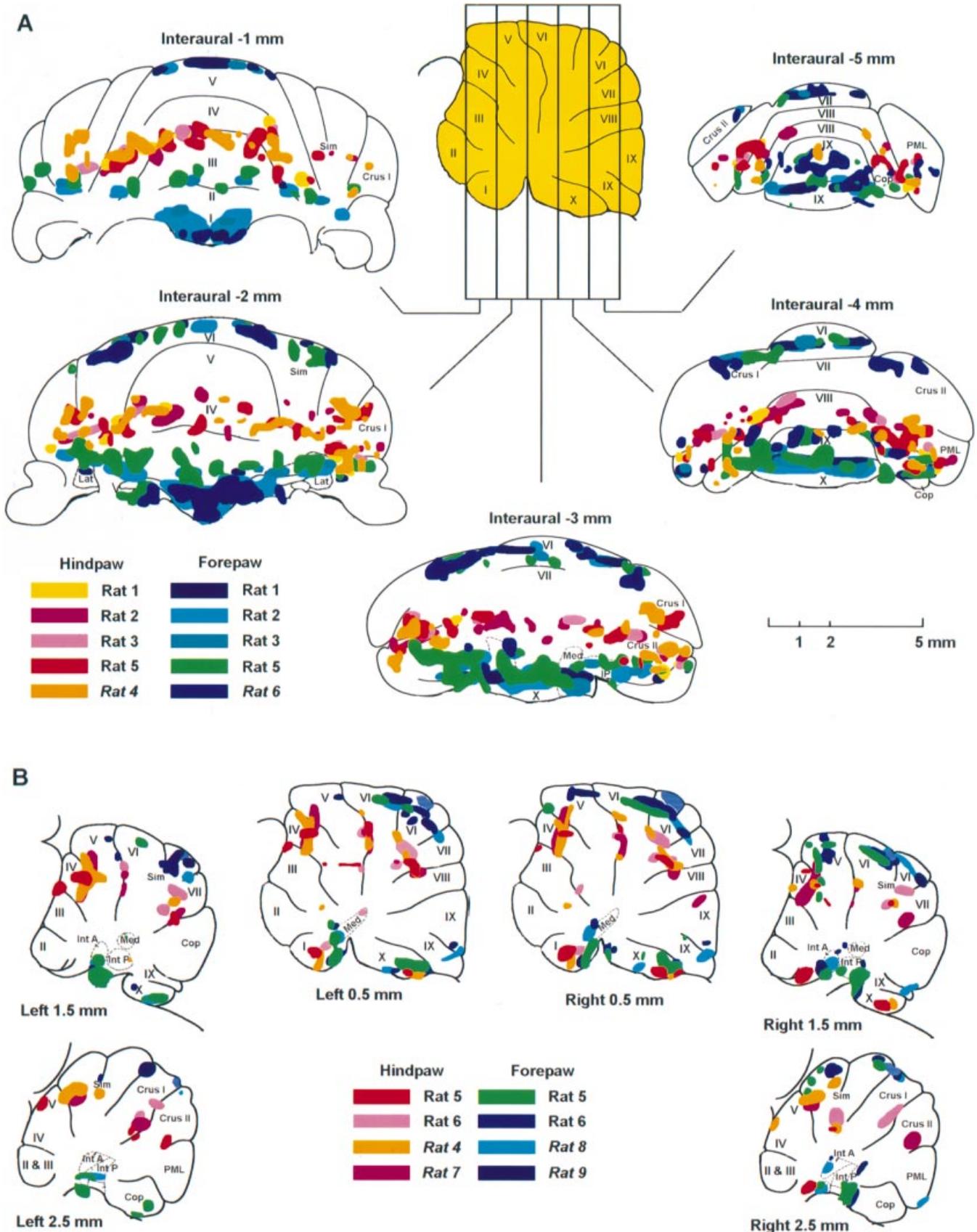
FIG. 3. Composite maps of areas activated during hindpaw and forepaw stimulation, from all the imaged rat cerebella. (A) Coronal images. (B) Sagittal images. The red-tinted spots show activated areas resulting from hindpaw stimulation and those that are blue-green tinted result from forepaw stimulation. After hind- or forepaw stimulation, several commonly activated areas are present in the different animals, with a clear separation of the fore- and hindpaw areas in the rostral cerebellum. The activated areas shown in this figure were thresholded at a t-value level of 2.0.
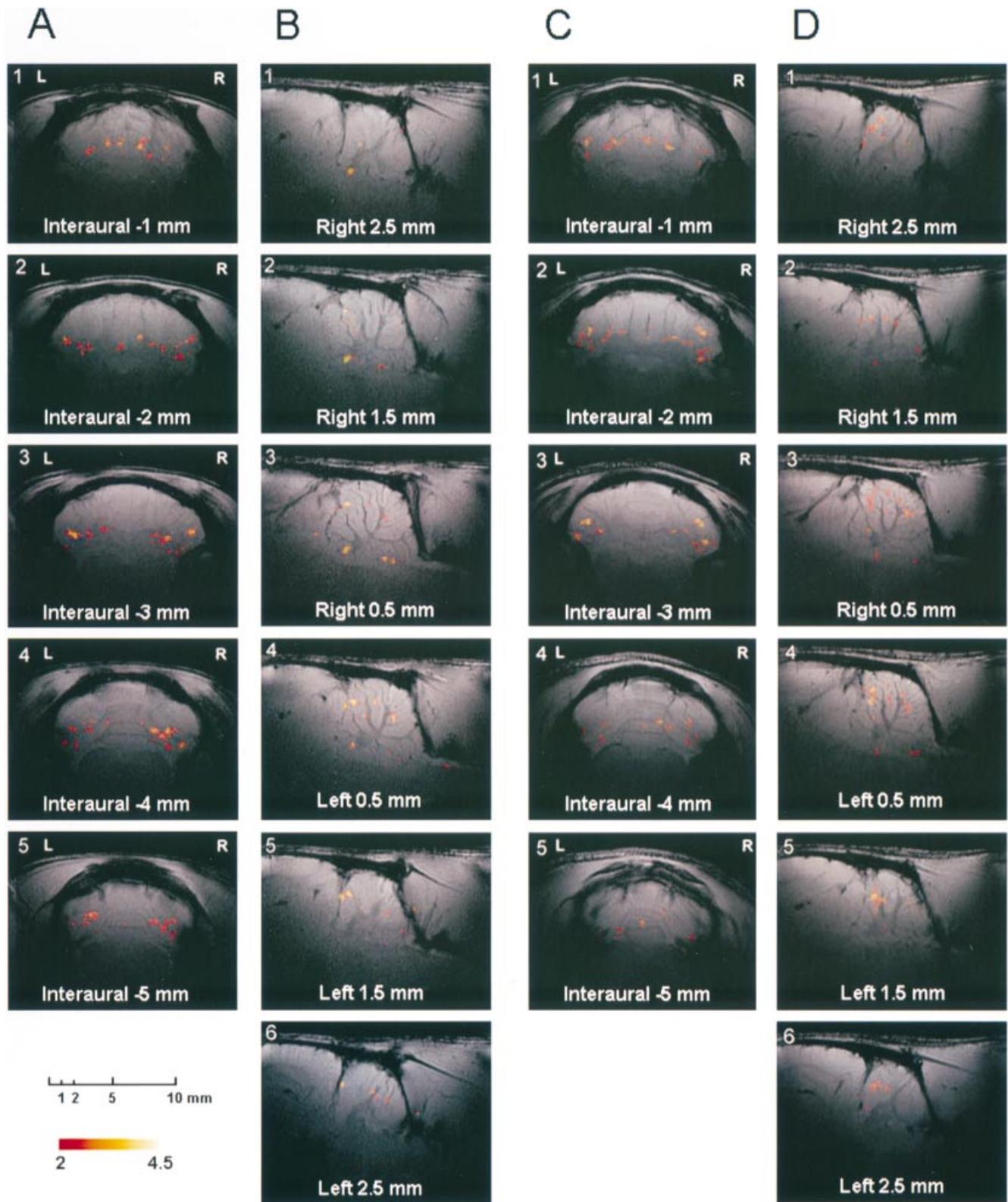
FIG. 4. Cerebellar activation maps resulting from electrical stimulation of the left hindpaw superimposed on high-resolution images of the cerebellum. A and B are from rat 5 while C and D are from rat 4. Coronal images (A and C) show five consecutive 1-mm-thick slices located from –1 to –5 mm interaurally. Sagittal images (B and D) show six slices of 1-mm thickness. Several of the activated areas in 4B and D match with the position of the activations in the coronal images in 4A and C. All activations are computed from a functional image set of 36 images (except 4A, from 32 images) and are shown in a colour code representing *t*-values ranging from 2.0 to 4.5.
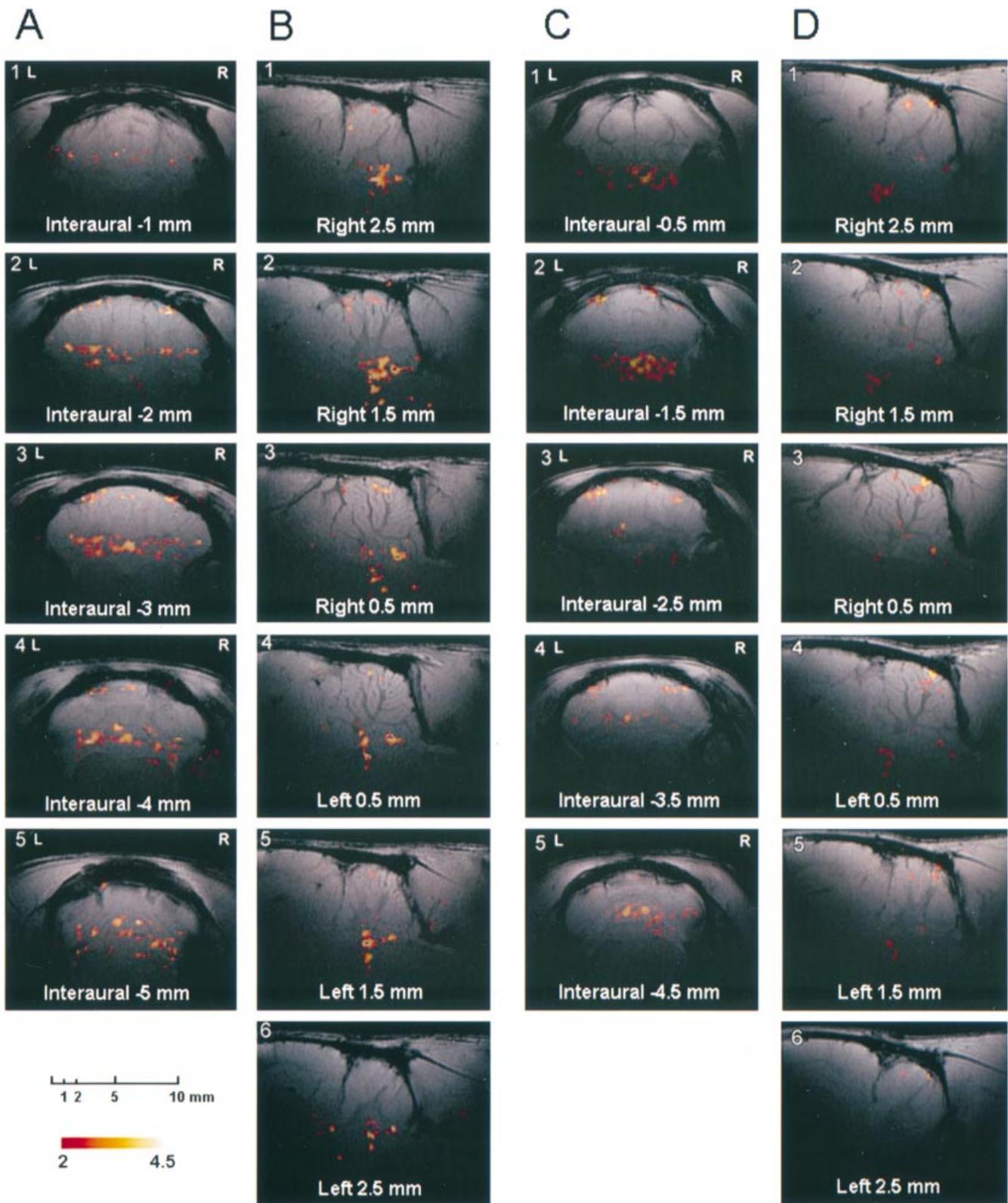
FIG. 5. Cerebellar activation maps resulting from electrical stimulation of the left forepaw. A and B are from rat 5 while C and D are from rat 6. Same conventions as in Fig. 4.

In the posterior cerebellum, a spot is seen deep in lobule VIa close to the primary fissure in the sagittal images, mostly ipsilateral central in rat 5 (B3 and 4) and more extensive in rat 4 (D2–4, with a second higher spot of activation in D3), but these activations are not significant in the corresponding coronal images (A3 and C3) except for the ipsilateral spot in A3 (it was also visible in the corresponding images of rats 2 and 3; cf. Fig. 3A).

Similarly, an activation is observed deep in VIb in the sagittal images of rat 4 only (D3 and 4).

Another activation in the posterior cerebellum is deep in lobules VII and VIII, close to the prepyramidal fissure. We find this as extensive bilateral spots in sagittal images B3–5 and D2–5, and as two symmetric activations in A4 or as two contralateral spots in C4. More laterally, several spots of activation are visible on each side of the coronal images A4 and A5, and C4 and C5, in the copula pyramis and lower paramedian lobule; these activations are mostly outside the field of view of the sagittal images except for a small ipsilateral activation in B6 and a contralateral one in D1.

Finally, one (C5, D3–4) or two (B3–4) medial activations are seen in lobule X close to the posterolateral fissure.

Cerebellar activation caused by left forepaw stimulation

Stimulation of the left forepaw (Fig. 5) gave rise to signal changes in parts of the cerebellum different from those seen during the hindpaw stimulation. This stimulation also resulted in a bilateral pattern of activation, which was confined to two horizontal levels: a rostral series of spots 0.5–1.5 mm below the surface of the rostral vermis and paravermis, and extensive activations in the caudal cerebellum and brainstem. The latter activation was typical for the forepaw stimulation paradigm; it was seen in all seven rats, while no brainstem activation was found for the hindpaw stimulation in any of the same rats. Though this brainstem activation was very reproducible, it did not seem very reliable; the activations were very large, often spanning several structures and were sometimes located in unlikely places (e.g. the vestibular nucleus and cerebellar peduncles). As these activations were specific to one stimulation paradigm they were probably genuine, but they could not be resolved accurately because of the large distances from the surface coil. We will therefore describe the cerebellar locations only.

In coronal slice A1, several spots of activation are seen in a mediolateral band, with more pronounced activation ipsilaterally. These activations were common to all rats (Fig. 3A) except for rat 6, presumably because of the more anterior positioning of the first coronal slice in this rat (Fig. 5C). These activations could not be found in the sagittal images, except for an activation deep in lobule IV in rat 5 (B1 and 2).

Additional activations in the anterior cerebellum were located superficially in lobules IV and V of the vermis; several symmetrically disposed patches of activation span mediolaterally along the upper part of coronal slice A2 and C2. In the sagittal images, the contralateral activations can be located more easily: superficial (B2 and 3) in lobule IV and several spots in lobule V close to the primary fissure (B2, D1–3 and D6).

In the posterior lobe several patches were located in lobule VI: in VIa close to the primary fissure (B2–4), in VIa/b at the fissure (B2–4 and D2–6) and in VIb (B2–3 and D3–6). Note that on sagittal slices B2 and B3, right of the midline, these activations seemed to form a continuous sagittal band (*t*-value of 3.4), but this is not the case on D2–3. All these activations were in olivary termination zone A (Buisseret-Delmas & Angaut, 1993). The coronal images revealed activations corresponding to the possible sagittal band just described in the midline region of lobule VI of the vermis (A3, A4 and C5). Additionally, several more lateral spots of activation were found in lobule VI (A3–5, C3 and C4). Here more patches were activated ipsilaterally, and the most contralateral ones had a symmetric ipsilateral homologue. All the sagittal images from rat 6 show, additionally, a highly significant activation at the upper surface of lobule VIb (D1–6, grey patch in Fig. 3B) which is likely to be a venous artifact caused by one of the veins covering the cerebellum.

As mentioned before, the forepaw stimulation also activated large parts of the lower cerebellum which could not be resolved accurately. These included parts of the lower vermis, with several activations in the midline of lobule I (A2, A3, B3, B4, C2 and C3) and seemingly even more extensive in lobule X (A4, A5, B2–5, C5 and D2–5) close to the posterolateral fissure bilaterally. More laterally, activations were found in the copula pyramis and the paramedian lobule, mostly contralaterally (A4, A5, B1, B6, C4 and C5). The forepaw stimulation may also have activated the cerebellar nuclei, but these activations are not very well delineated. Specifically, in coronal slices A2/C2 and A3/C3 most of the caudal activity may be located in the medial (B3, B4 and D3), interpositus (B1, B2, B5, B6, D1 and D2) and lateral nuclei.

Discussion

We have demonstrated that the activation pattern observed in the rat cerebellum during electrical stimulation of a paw was very patchy and showed an unexpected horizontal organization. Before discussing the implications of our findings, we will first consider technical aspects related to our stimulation and imaging protocols. Next we will show that several of the activations we observed largely match the known anatomical projections.

Comparisons with other animal fMRI studies

The regions of signal elevation in the somatosensory cortex during electrical stimulation of the left fore- and hindpaw in this study corresponded to the front and hindlimb regions in rat cortex (Chapin & Lin, 1990) and to activations described in other fMRI studies (Hyder *et al.*, 1994; Gyngell *et al.*, 1996; Kerskens *et al.*, 1996). Overall, the activated areas were smaller than those found in other studies in which electrical stimulation of the forepaw was used. The discrepancy might be due to the lower current used. Gyngell *et al.* (1996) used a current of 0.5 mA, which is 2.5 × higher than the one we used, while Hyder *et al.* (1994) used a voltage-controlled stimulator, so that they did not report the stimulation current. Gyngell *et al.* (1996) also reported a size discrepancy between these two studies, which was attributed to the stimulation current they used.

We used a surface coil because preliminary fMRI tests with a volume birdcage coil, which has a lower signal-to-noise ratio than the surface coil, resulted in no detectable signal changes above threshold after stimulation. Disadvantages of using the surface coil are that the detectable area is relatively small and there is a signal drop (the further away from the midpoint of the sphere the larger the signal drop, see Figs 4 and 5). This can be partially resolved by using adiabatic pulses. For these reasons it was not possible to image the cortex and the cerebellum at the same time, as the structures are 12 mm apart. As we expected that hindlimb and forelimb projections could be found in the deep cerebellum (Voogd, 1995), we used a relatively large surface coil. In the cortex, however, the activated zones are positioned near the cortical surface, which makes it possible to use a smaller surface coil with a better signal-to-noise ratio; for example, Hyder *et al.* (1994) used a surface coil with a diameter of 8 mm.

Validity and reproducibility of the observed activations

With fMRI of neural responses, the signal change observed may sometimes reflect the presence of a large venous blood vessel in the neighbourhood instead of being truly representative of neural activation (Ogawa *et al.*, 1990a,b; Segebarth *et al.*, 1994). In Fig. 2 the activations at the cortical surfaces centrally between the two hemispheres were due to such a large venous blood vessel (the

sagittal sinus). Similar signals of venous origin have been reported in other studies of rat cortical responses (Hyder *et al*., 1994; Kerskens *et al*., 1996). In the cerebellum this problem is less likely to occur because of the absence of large veins on the top of or inside the cerebellum (Scremin, 1995). We also had the advantage of using a 7-T high-strength field, which results in a relatively small contribution from large vessels (vs. capillaries) in the T_2^*-signal changes compared with the lower fields used in human studies (Menon *et al*., 1995). Because we did not see any cerebellar activation common to the forepaw and hindpaw stimulation paradigms, we assume that most cerebellar activations reflect neural activity. An exception is the very superficial activation in Fig. 5D. It is also possible that the activations caused by forepaw or hindpaw stimulation which we attributed to lobule X were in fact due to the venous plexus beneath this lobule.

The reproducibility of the cerebellar activations was not perfect. The composite images in Fig. 3 demonstrate that while most activation spots were present in all of the rats imaged, they were not always localized in exactly the same place. Some of these differences could be explained by the variability in positioning of the slices between rats and by the volume effects due to the relatively thick slices (1 mm, which is also the most likely cause of differences between the sagittal and coronal images), but it is likely that genuine differences were present between individual rats. Most of these differences may be caused by the normal variability in the gross anatomy of the brain, which is already obvious when the two rat brains shown in Figs 4 and 5 each are compared [see also Perciavalle *et al*. (1998) for variability in sizes of the cat cerebellum and Steinmetz & Seitz (1991), Woods *et al*. (1994), Rombouts *et al*. (1997) and Strother *et al*. (1997) for variability among human brains]. In humans these differences can be corrected for by transforming each image to a standard human brain (Talairach & Tournoux, 1988), but such techniques are not available for the rat brain. As a consequence the exact anatomical localizations as shown in the composites in Fig. 3 have to be considered approximate, and it is not known if the small differences in patch localizations between rats are genuine or would disappear after normalization.

Anatomical projections to the cerebellum

The fMRI images usually had insufficient resolution to distinguish between activations in the molecular vs. granular layer of the cerebellar cortex. This is important because such localization would identify the source of the activation; granular layer activations can be caused by mossy fibre input only, while an isolated molecular layer activation would suggest input from climbing fibres. Some isolated evidence for both can be found in the sagittal images of Fig. 5B, where the rostral activations in the anterior lobe (slices 2–4) had both very superficial (presumably molecular layer) and deeper (presumably granular layer) components, while the activations in lobule VI were often only in the superficial layers (e.g. slice 4).

For now we can only compare the activated regions with the known somatosensory projections to the cerebellum. Of these, only the mossy fibre projections from the spinocerebellar and cuneocerebellar pathways and an indirect spinocerebellar path through the lateral reticular nucleus have been described in detail in the rat (Voogd, 1995). These projections have sometimes been described as following the parasagittal banding revealed by zebrin II immunocytochemistry (Ji & Hawkes, 1994), but many studies (reviewed by Voogd, 1995) have found a less strict organization.

The spinocerebellar pathways which are activated during hindpaw stimulation project not only to the vermis of lobules II, III, IV and V (Tolbert *et al*., 1993; Voogd, 1995) like the activations we found, but

also to lobule II (Matsushita *et al*., 1991; Tolbert *et al*., 1993; Alisky & Tolbert, 1997), where we detected no significant activation. Similarly, in the posterior lobe, projections to lobule VIII have been described (Gravel & Hawkes, 1990; Matsushita *et al*., 1991) consistent with our observations. Conversely, we also observed activations in lobules VI and in lobule X, which are not known projection zones of the direct spinocerebellar pathway (see also the remarks above about the veracity of the lobule X activations). These activations could be caused by other projections arising from many different brain structures, though the most likely ones are the lateral nucleus (Clendenin *et al*., 1974b; Russchen *et al*., 1976; Chan-Palay *et al*., 1977), the olivary nuclei (Voogd, 1995) and the corticopontine projection for the more lateral activations (Brodal & Bjaalie, 1997). The topography of the corticopontine input to the rat cerebellum has not been described in detail, but in the case of facial inputs it is known to be activated during somatosensory activation (Bower *et al*., 1981) and to be more bilateral in its projections than the trigeminal mossy fibre input (Morissette & Bower, 1996).

The cuneocerebellar pathways which were activated by the forepaw stimulation project to the anterior vermis in an ipsilateral sagittal band spanning lobules II to V and consisting of several separated patches (Alisky & Tolbert, 1997; Tolbert & Gutting, 1997). We found bilateral activations in lobules III-V. This is not in contradiction with the anatomical data, as weak staining was also found at the contralateral side (Tolbert & Gutting, 1997). Moreover, similar to the mentioned anatomical study, we observed a mediolateral band of activations in the posterior part of lobule V (Fig. 5A2 and C2), which was more pronounced ipsilaterally. Finally, the bilateral midline activations in lobule I again match the anatomical projections (Tolbert & Gutting, 1997) where, similar to our observation of rostral and caudal horizontal planes of activation, the terminals in lobule I are completely separated from the projections to the more rostral lobules.

The cuneocerebellar projection to the posterior lobe forms transversely orientated bands (Tolbert & Gutting, 1997) which fits our observations. Nevertheless, in lobule VI only an ipsilateral band has been described in VIa, while we found bilateral activations in both VIa and VIb. One explanation for this discrepancy could, of course, be the possible contralateral parasagittal band observed in several rats (Fig. 3B), suggestive of the activation of climbing fibres originating in medial subnucleus C of the medial accessory olive (Buisseret-Delmas & Angaut, 1993). Another possible source of bilateral projections is the lateral reticular nucleus, especially if it was activated by the bilateral ventral flexor reflex tract (Clendenin *et al*., 1974a,c). More laterally, the lobule VI activations were mainly ipsilateral, like the mossy fibre projections (Tolbert & Gutting, 1997). These authors also describe two more posterior transverse bands of mossy fibre projections, one extending into the paramedian lobule and another one into the copula pyramis. The ipsilateral forelimb projection to the paramedian lobule has also been described in electrophysiological studies (Welker, 1987; the copula pyramis was not investigated). We found extensive activations in both the paramedian lobule and copula pyramis, but again these were bilateral while the known anatomical projections are to the ipsilateral hemisphere and the bilateral vermis only.

The more extensive activations in the cerebellar nuclei during forelimb compared with hindlimb stimulation (Fig. 3B) fit with electrophysiological studies that have described an extensive representation of the forelimb (and the face) in the rat dentate nucleus, with only a small representation of the hindlimb (Angaut & Cicirata, 1990). Unfortunately, as was mentioned before, the lower

resolution of the images at this distance from the surface coil did not allow for an accurate anatomical localization of the nuclear activity.

A final point concerning the correspondence with anatomical studies of the mossy fibre system is that these investigations have shown a clear separation between the spino- and cuneocerebellar projections to the anterior lobe (Ji & Hawkes, 1994; Alisky & Tolbert, 1997). Similarly, we found completely distinct activation sites during hindpaw and forepaw stimulation (Fig. 3), but while the anatomical studies found a mediolateral separation we usually observed a rostrocaudal one. Careful inspection of the data of rat 5 (Figs 4A and 5A) reflects, however, that the forepaw and hindpaw activations were often also separated mediolaterally.

The patchy mediolateral organization in horizontal planes

Both transverse and longitudinal patterns of organization are present in the anatomy of the cerebellum (Ito, 1984; Voogd & Ruigrok, 1997). The transverse axis is determined by the parallel fibres and their relationship with the dendritic arbours in the molecular layer (Braitenberg & Atwood, 1958). In most of the cerebellum, the parallel fibres form an uninterrupted transverse band from the vermis to the most lateral hemisphere (Voogd, 1995). This has led Eccles *et al.* (1967) to propose that beams of parallel fibre activation would be the fundamental mode of cerebellar operation. Later authors were struck by the longitudinal zonal organization of the corticonuclear projections, which was found to match the parasagittal organization of the climbing fibre projections (Voogd & Bigare, 1980; Voogd, 1995). This strong parasagittal organization of one afferent pathway and of the only efferent pathway of cortex has been proposed to be further subdivided into microzones (Oscarsson, 1979). The parasagittal organization can also be found in the banding of the cerebellum produced with several staining techniques (Hawkes & Gravel, 1991). Whether the second afferent system, the mossy fibre system, follows a similar pattern of parasagittal organization is controversial (Tolbert *et al.*, 1993; Ji & Hawkes, 1994; Voogd, 1995; Tolbert & Gutting, 1997).

Neither of these two forms of organization were found, however, in careful electrophysiological studies of granular layer activation by somatosensory mossy fibre input (Shambes *et al.*, 1978; Welker, 1987; Bower & Kassel, 1990). Instead, these authors found what they called a fractured somatotopy; each body location was represented many times in a mosaic of patches which were mixed in a seemingly random order. Moreover, when Purkinje cell responses were recorded, similar patch-like receptive fields were found, instead of the expected beam-like responses due to parallel fibre activation (Bower & Woolston, 1983). This patchy activation of cerebellar cortex by mossy fibre stimulation has also been observed in voltage imaging of the isolated guinea pig cerebellum (Cohen & Yarom, 1998).

The few human fMRI studies of the somatotopic organization of the cerebellum have revealed a mixture of activation patterns during motor activity, including parasagittal bands (Ellerman *et al.*, 1994), mediolateral bands (Ellerman *et al.*, 1994; Nitschke *et al.*, 1996) and many isolated patches (Ellerman *et al.*, 1994; Nitschke *et al.*, 1996). In our study we found all of these activation patterns during low amplitude electrical stimulation of a rat paw too, with a predominance of isolated patches and mediolateral bands. The most striking pattern, however, was a rostrocaudal horizontal organization of these responses. This is most obvious in the sagittal images (e.g. Fig. 3B), where most activations lie in either a rostral or caudal plane with a width of 1–1.5 mm. The rostral planes were more obvious, because they were completely separate for fore- and hindpaw stimulation. They comprise activations in both anterior (lobules III–V) and

posterior (VI–VIII) cerebellum. The caudal planes were not separated and probably included nuclear activations, but, as mentioned before, the image resolution was poor at this depth.

We are not aware of any previous description of such a horizontal organization in the cerebellar cortex. As we pointed out above, many of the observed activations correspond to known anatomical projection sites of spinocerebellar and cuneocerebellar mossy fibres, which also have a patchy organization (Tolbert *et al.*, 1993; Tolbert & Gutting, 1997). These studies all rely on the injection of tracers into the spinal cord, which even in the case of very small injections is not expected to label fibres which carry sensory information from a small body surface, like a single paw, specifically. Therefore it is not surprising that anatomical tracer studies show a much wider projection area than observed in our fMRI study. Similarly, most electrophysiological studies would never have found a horizontal organization because they either mapped activity at the surface of the hemispheres (Shambes *et al.*, 1978) or vermis (Joseph *et al.*, 1978) only, or made penetrations in one lobule only (e.g. the many studies summarized by Ito (1984)).

Obviously our observation of a horizontal organization needs confirmation, both by recording from the sites of activation in electrophysiological studies and by demonstrating that this pattern is not specific to the electrical activation of the paws. Our study also shows the importance of taking slices of the cerebellum at multiple orientations, as some activations in the coronal slices seemed to be parasagittal bands but were really isolated patches, while the sagittal slices did not demonstrate the mediolateral bands clearly.

The functional significance of the observed pattern of activation raises interesting questions. The mediolateral organization of bands and patches within one coronal slice probably follows the corresponding parallel fibre beams. Several theories of cerebellar function suggest that multiple activation sites along one beam would allow mixtures of different input which may be important for Purkinje cell functioning (Bower, 1997; Braitenberg *et al.*, 1997; De Schutter, 1998). Whether the organization of these mediolateral bands within one broad horizontal plane throughout different lobules has a functional significance, or reflects the developmental patterns (Oberdick *et al.*, 1998) only, is still unknown.

Abbreviations

Acknowledgements

References

Alisky, J.M. & Tolbert, D.L. (1997) Quantitative-analysis of converging spinal and cuneate mossy fiber afferent-projections to the rat cerebellar anterior lobe. *Neuroscience*, **80**, 373–388.

Allen, G., Buxton, R.B., Wong, E.C. & Courchesne, E. (1997) Attentional activation of the cerebellum independent of motor involvement. *Science*, **275**, 1940–1943.

Angaut, P. & Cicirata, F. (1990) Dentate control pathways of cortical motor activity. Anatomical and physiological studies in rat: comparative considerations. *Arch. Ital. Biol.*, **128**, 315–330.

Binder, J.R. (1997) Neuroanatomy of language processing studied with functional MRI. *Clin. Neurosci.*, **4**, 87–94.

Bower, J.M. (1997) Is the cerebellum sensory for motor's sake or motor for sensory's sake: the view from the whiskers of a rat? *Prog. Brain Res.*, **114**, 463–496.

Bower, J.M., Beerman, D.H., Gibson, J.M., Shambes, G.M. & Welker, W. (1981) Principles of organization of a cerebro-cerebellar circuit. Micromapping the projections from cerebral (SI) to cerebellar (granule cell layer) tactile areas of rats. *Brain Behav. Evol.*, **18**, 1–18.

Bower, J.M. & Kassel, J. (1990) Variability in tactile projection patterns to cerebellar folia crus IIA of the Norway rat. *J. Comp Neurol.*, **302**, 768–778.

Bower, J.M. & Woolston, D.C. (1983) Congruence of spatial organization of tactile projections to granule cell and Purkinje cell layers of cerebellar hemispheres of the albino rat: vertical organization of cerebellar cortex. *J. Neurophysiol.*, **49**, 745–766.

Braitenberg, V. & Atwood, R.P. (1958) Morphological observations on the cerebellar cortex. *J. Comp Neurol.*, **109**, 1–33.

Braitenberg, V., Heck, D. & Sultan, F. (1997) The detection and generation of sequences as a key to cerebellar function. Experiments and theory. *Behav. Brain Sci.*, **20**, 229–245.

Brodal, P & Bjaalie, J.G. (1997) Salient anatomic features of the cortico-ponto-cerebellar pathway. *Prog. Brain Res.*, **14**, 227–249.

Buisseret-Delmas, C. & Angaut, P. (1993) The cerebellar olivo-corticonuclear connections in the rat. *Prog. Neurobiol.*, **40**, 63–87.

Chan-Palay, V., Palay, S.L., Brown, J.T. & Van Itallie, C. (1977) Sagittal organization of olivocerebellar and reticulocerebellar projections: autoradiographic studies with 35S-methionine. *Exp. Brain Res.*, **30**, 561–576.

Chapin, J.K. & Lin, C.-S. (1990) The somatic sensory cortex of the rat. In Kolb, B. & Tees, R.C. (eds), *The Cerebral Cortex of the Rat*. The MIT Press, Cambridge, MA, pp. 341–380.

Chen, G., Hanson, C.L. & Ebner, T.J. (1996) Functional parasagittal compartments in the rat cerebellar cortex: an *in vivo* imaging study using neutral red. *J. Neurophysiol.*, **76**, 4169–4174.

Clendenin, M., Ekerot, C.F. & Oscarsson, O. (1974a) The lateral reticular nucleus in the cat. III. Organization of component activated from ipsilateral forelimb tract. *Exp. Brain Res.*, **21**, 501–513.

Clendenin, M., Ekerot, C.F., Oscarsson, O. & Rosen, I. (1974b) The lateral reticular nucleus in the cat. I. Mossy fibre distribution in cerebellar cortex. *Exp. Brain Res.*, **21**, 473–486.

Clendenin, M., Ekerot, C.F., Oscarsson, O. & Rosen, I. (1974c) The lateral reticular nucleus in the cat. II. Organization of component activated from bilateral ventral flexor reflex tract (bVFRT). *Exp. Brain Res.*, **21**, 487–500.

Cohen, D. & Yarom, Y. (1998) Patches of synchronized activity in the cerebellar cortex evoked by mossy-fiber stimulation: questioning the role of parallel fibers. *Proc. Natl Acad. Sci. USA*, **98**, 15032–15036.

De Schutter, E. (1998) Dendritic voltage and calcium-gated channels amplify the variability of postsynaptic responses in a Purkinje cell model. *J. Neurophysiol.*, **80**, 504–519.

De Schutter, E. & Maex, R. (1996) The cerebellum: cortical processing and theory. *Curr. Opin. Neurobiol.*, **6**, 759–764.

De Zeeuw, C.I., Lang, E.J., Sugihara, I., Ruigrok, T.J.H., Eisenman, L.M., Mugnaini, E. & Llinás, R. (1996) Morphological correlates of bilateral synchrony in the rat cerebellar cortex. *J. Neurosci.*, **16**, 3412–3426.

Desmond, J.E. & Fiez, J.A. (1998) Neuroimaging studies of the cerebellum: language, learning and memory. *Trends Cogn. Sci.*, **2**, 355–362.

Ebner, T.J. & Chen, G. (1995) Use of voltage-sensitive dyes and optical recordings in the central-nervous-system. *Prog. Neurobiol.*, **46**, 463–506.

Eccles, J.C., Ito, M. & Szentagothai, J. (1967) *The Cerebellum as a Neuronal Machine*. Springer-Verlag, Berlin.

Ellerman, J.M., Flament, D., Kim, S.-G., Fu, Q.-G., Merkle, H., Ebner, T.J. & Ugurbil, K. (1994) Spatial patterns of functional activation of the cerebellum investigated using high field (4T) MRI. *NMR Biomed.*, **7**, 63–68.

Gao, J.H., Parsons, L.M., Bower, J.M., Xiong, J.H., Li, J.Q. & Fox, P.T. (1996) Cerebellum implicated in sensory acquisition and discrimination rather than motor control. *Science*, **272**, 545–547.

Gravel, C. & Hawkes, R. (1990) Parasagittal organization of the rat cerebellar cortex: direct comparison of Purkinje cell compartments and the organization of the spinocerebellar projection. *J. Comp. Neurol.*, **291**, 79–102.

Gyngell, M.L., Bock, C., Schmitz, B., Hoehn-Berlage, M. & Hossmann, K.-A. (1996) Variation of functional MRI signal in response to frequency of somatosensory stimulation in a-chloralose anesthetized rats. *Magn. Res. Med.*, **36**, 13–15.

Handwerker, H.O. & Kobal, G. (1993) Psychophysiology of experimentally induced pain. *Physiol. Rev.*, **73**, 639–671.

Hawkes, R. (1997) An anatomical model of cerebellar modules. *Prog. Brain Res.*, **114**, 39–52.

Hawkes, R. & Gravel, C. (1991) The modular cerebellum. *Prog. Neurobiol.*, **36**, 309–327.

Huang, W., Palyka, I., Li, H., Eisenstein, E.M., Volkow, N.D. & Springer, C.S. Jr (1996) Magnetic resonance imaging (MRI) detection of the murine brain response to light: temporal differentiation and negative functional MRI changes. *Proc. Natl Acad. Sci. USA*, **93**, 6037–6042.

Hyder, F., Behar, K.L., Martin, M.A., Blamire, A.M. & Shulman, R.G. (1994) Dynamic magnetic resonance imaging of the rat brain during forepaw stimulation. *J. Cereb. Blood Flow Metab.*, **14**, 649–655.

Ito, M. (1984) *The Cerebellum and Neural Control*. Raven Press, New York.

Jezzard, P., Rauschecker, J.P. & Malonek, D. (1997) An *in vivo* model for functional MRI in cat visual cortex. *Magn. Res. Med.*, **38**, 699–705.

Ji, Z. & Hawkes, R. (1994) Topography of Purkinje cell compartments and mossy fiber terminal fields in lobule II and lobule III of the rat cerebellar cortex: spinocerebellar and cuneocerebellar projections. *Neuroscience*, **61**, 935–954.

Joseph, J.W., Shambes, G.M., Gibson, J.M. & Welker, W. (1978) Tactile projections to granule cells in caudal vermis of the rat's cerebellum. *Brain Behav. Evol.*, **15**, 141–149.

Karni, A., Meyer, G., Jezzard, P., Adams, M.M., Turner, R. & Ungerleider, L.G. (1995) Functional MRI evidence for adult motor cortex plasticity during motor skill learning. *Nature*, **377**, 155–158.

Kerskens, C.M., Hoehn-Berlage, M., Schmitz, B., Bush, E., Bock, C., Gyngell, M.L. & Hossmann, K.-A. (1996) Ultrafast perfusion-weighted MRI of functional brain activation in rats during forepaw stimulation: comparison with T_2^*-weighted MRI. *NMR Biomed.*, **8**, 20–23.

Matsushita, M., Ragnarson, B. & Grant, G. (1991) Topographic relationship between sagittal Purkinje cell bands revealed by a monoclonal antibody to zebrin i and spinocerebellar projections arising from the central cervical nucleus in the rat. *Exp. Brain Res.*, **84**, 133–141.

Menon, R.S., Kim, S.G., Hu, X., Ogawa, M. & Ugurbil, K. (1995) Functional MR imaging using the BOLD approach: field strength and sequence issues. In Le Bihan, D. (ed.), *Diffusion and Perfusion Magnetic Resonance Imaging*. Raven Press, New York, pp. 327–344.

Morissette, J. & Bower, J.M. (1996) Contribution of somatosensory cortex to responses in the rat cerebellar cortex granule cell layer following peripheral tactile stimulation. *Exp. Brain Res.*, **109**, 240–250.

Nitschke, M.F., Kleinschmidt, A., Wessel, K. & Frahm, J. (1996) Somatotopic motor representation in the human anterior cerebellum. A high-resolution functional MRI study. *Brain*, **119**, 1023–1029.

Oberdick, J., Baader, S.L. & Schilling, K. (1998) From zebra stripes to postal zones: deciphering patterns of gene expression in the cerebellum. *Trends Neurosci.*, **21**, 383–390.

Ogawa, S., Lee, T.M., Kay, A.R. & Tank, D.W. (1990a) Brain magnetic resonance imaging with contrast dependent on blood oxygenation. *Proc. Natl Acad. Sci. USA*, **87**, 9868–9882.

Ogawa, S., Lee, T.M., Nayak, A.S. & Glynn, P. (1990b) Oxygenation-sensitive contrast in magnetic resonance imaging of rodent brain at high magnetic fields. *Magn. Res. Med.*, **14**, 68–78.

Oscarsson, O. (1979) Functional units of the cerebllum: sagittal zones and microzones. *Trends Neurosci.*, **2**, 143–145.

Paxinos, G. & Watson, C. (1986) *The Rat Brain in Stereotaxic Coordinates*. Academic Press, San Diego.

Peeters, R.R., Verhoye, M., Van Der Linden, A., Van Dyck, D., Vos, B.P. & De Schutter, E. (1998) Functional imaging resonance imaging of the rat cerebellum during electrical stimulation of the fore- and hindpaw at 7 tesla. *Eur. J. Neurosci.*, **10** (Suppl. 10), 438.

Perciavalle, V., Bosco, G. & Poppele, R.E. (1998) Spatial organization of proprioception in the cat spinocerebellum. Purkinje cell responses to passive foot rotation. *Eur. J. Neurosci.*, **10**, 1975–1985.

Raymond, J.L., Lisberger, S.G. & Mauk, M.D. (1996) The cerebellum: a neuronal learning machine? *Science*, **272**, 1126–1131.

Rombouts, S.A., Barkhof, F., Hoogenraad, F.G., Sprenger, M., Valk, J. & Scheltens, P. (1997) Test–retest analysis with functional MR of the activated area in the human visual cortex. *Am. J. Neuroradiol.*, **18**, 1317–1322.

Russchen, F.T., Groenewegen, H.J. & Voogd, J. (1976) Reticulocerebellar connections in the cat. An autoradiographic study. *Acta Morph. Neerl. Scand.*, **14**, 245–246.

Sakai, K., Watanabe, E., Onodera, Y., Itagaki, H., Yamamoto, E., Koizumi, H. & Miyashita, Y. (1995) Functional mapping of the human somatosensory cortex with echo-planar MRI. *Magn. Res. Med.*, **33**, 736–743.

Sasaki, K., Bower, J.M. & Llinás, R.R. (1989) Multiple Purkinje cell recording in rodent cerebellar cortex. *Eur. J. Neurosci.*, **1**, 572–586.

Schmahmann, J.D. (1997) *The cerebellum and cognition*, Vol. 41. Academic Press, San Diego.

Scremin, O.U. (1995) Cerebral vascular system. In Paxinos, G. (ed.), *The Rat Nervous System,* 2nd edn. Academic Press, San Diego,.

Segebarth, C., Belle, V., Delon, C., Massarelli, R., Decety, J., Lebas, J.F., Decorps, M. & Benabid, A.L. (1994) Functional MRI of the human brain: predominance of signals from extracerebral veins. *Neuroreport*, **5**, 813–816.

Shambes, G.M., Gibson, J.M. & Welker, W. (1978) Fractured somatotopy in granule cell tactile areas of rat cerebellar hemispheres revealed by micromapping. *Brain Behav. Evol.*, **15**, 94–140.

Steinmetz, H. & Seitz, R.J. (1991) Functional anatomy of language processing: neuroimaging and the problem of individual variability. *Neuropsychology*, **29**, 1149–1161.

Strother, S.C., Lange, N., Anderson, J.R., Schaper, K.A., Rehm, K., Hansen, L.K. & Rottenberg, D.A. (1997) Activation pattern reproducibility: measuring the effects of group size and data analysis models. *Hum. Brain Mapp.*, **5**, 312–316.

Talairach, J. & Tournoux, P. (1988) *Co-planar stereotaxic atlas of the human brain: 3-dimensional proportional system: an approach to cerebral imaging.* Thieme, Stuttgart.

Tolbert, D.L., Alisky, J.M. & Clark, B.R. (1993) Lower thoracic upper lumbar spinocerebellar projections in rats: a complex topography revealed in computer reconstructions of the unfolded anterior lobe. *Neuroscience*, **55**, 755–774.

Tolbert, D.L. & Gutting, J.C. (1997) Quantitative analysis of cuneocerebellar projections in rats: differential topography in the anterior and posterior lobes. *Neuroscience*, **80**, 359–371.

Tootell, R.B.H., Dale, A.M., Sereno, M.I. & Malach, R. (1996) New images from human visual cortex. *Trends Neurosci.*, **19**, 481–489.

Turner, R., Le Bihan, D., Moonen, C.T.W., DesPres, D. & Franck, J. (1991) Echo-planar time course MRI of cat brain oxygenation changes. *Magn. Res. Med.*, **22**, 159–166.

Voogd, J. (1995) Cerebellum. In Paxinos, G. (ed.), *The Rat Nervous System,* 2nd edn. Academic Press, San Diego, pp. 309–350.

Voogd, J. & Bigare, F. (1980) *Topographical distribution of olivary and cortico nuclear fibers in the cerebellum: a review.* In Courville, J.de Montigny, C. & Lamarre, Y. (eds), *The Inferior Olivary Nucleus: Anatomy and Physiology.* Raven Press, New York, pp. 207–235.

Voogd, J. & Ruigrok, T.J. (1997) Transverse and longitudinal patterns in the mammalian cerebellum. *Prog. Brain Res.*, **114**, 21–37.

Welker, W. (1987) Spatial organization of somatosensory projections to granule cell cerebellar cortex: functional and connectional implications of fractured somatotopy (summary of Wisconsin studies). In King, J.S. (ed.), *New Concepts in Cerebellar Neurobiology.* Alan R. Liss, New York, pp. 239–280.

Woods, R.P., Mazziotta, J.C. & Cherry, S.R. (1994) Optimizing activation methods: tomographic mapping of functional cerebral activity. In Thacher, R.W., Hallet, M., Zeffiro, T., John, E.R. & Huerta, M. (eds), *Functional Neuroimaging: Technical Foundations.* Academic Press, San Diego, pp. 47–58.

Yang, X., Hyder, F. & Shulman, R.G. (1996) Activation of single whisker barrel in rat brain localized by functional magnetic resonance imaging. *Proc. Natl Acad. Sci. USA*, **93**, 475–478.

Yang, X., Hyder, F. & Shulman, R.G. (1997) Functional MRI BOLD signal coincides with electrical activity in the rat whisker barrels. *Magn. Res. Med.*, **38**, 874–877.